Deformation in the lowermost mantle: linking seismic anisotropy, mineral physics and geodynamics

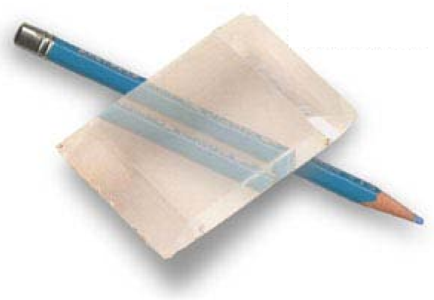

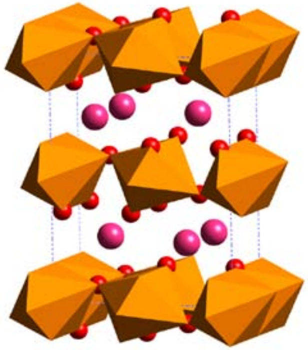

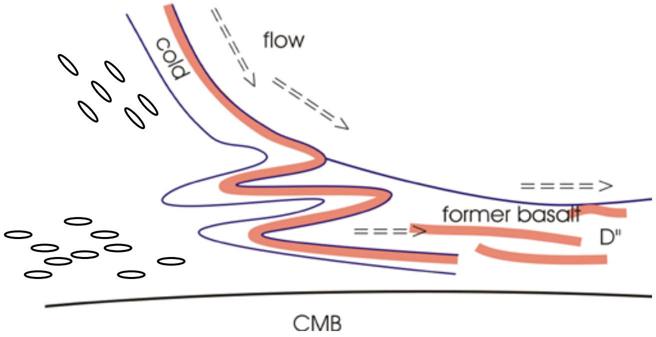

Michael Kendall

University of Bristol

Acknowledgements

- James Wookey - Bristol
- Andrew Walker - Bristol
- Andy Nowacki – Bristol
- Jack Walpole - Bristol
- Alessandro Forte – UQAM, Canada

COMITAC – ERC funding (PI - James Wookey)

University of BRISTOL

D” and the dynamics of the core and mantle

- Thermal boundary layer
- Site of plumes
- Birth of LLSVPs

- Resting place for slabs
- Boundary condition for core dynamics

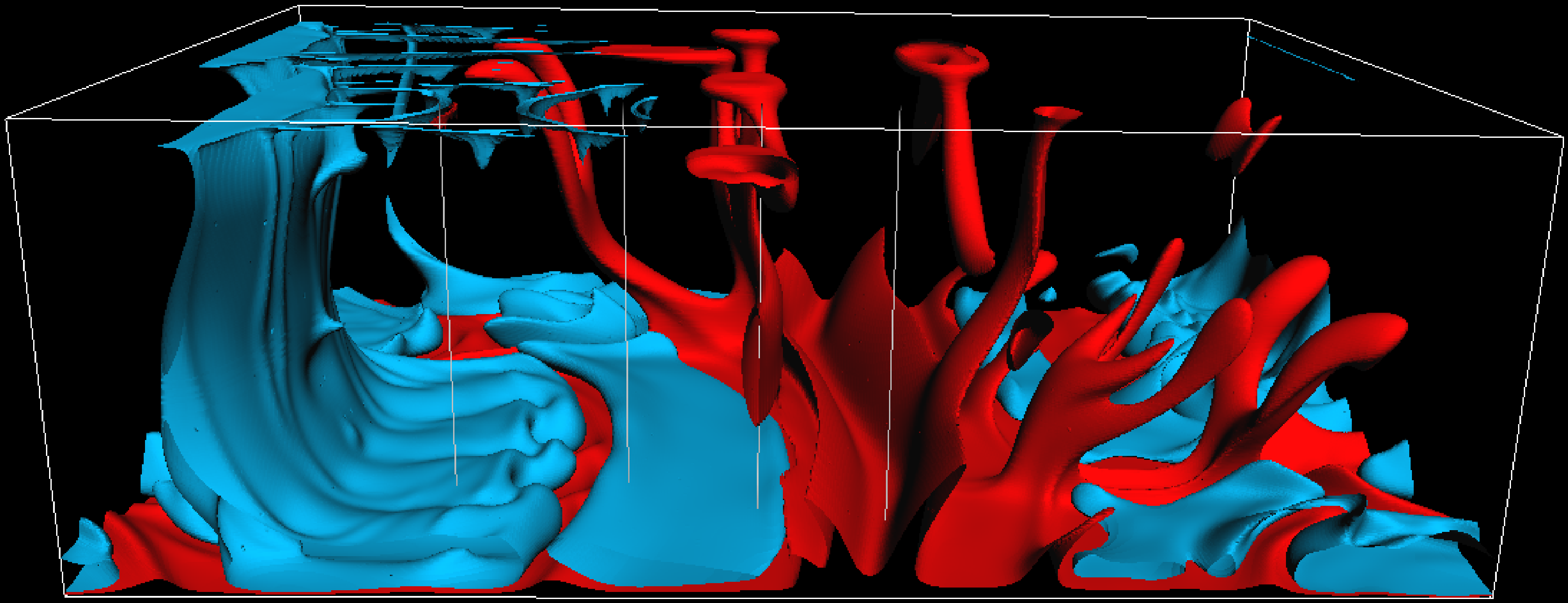

Mineralogy of the lower mantle

- Dominant mineral is perovskite
- Phase transition to post-perovskite

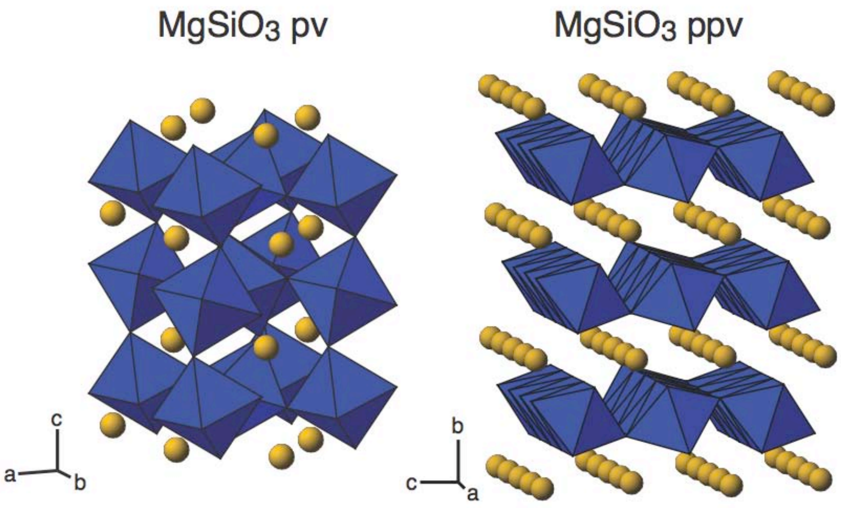

Tronnes, 2010

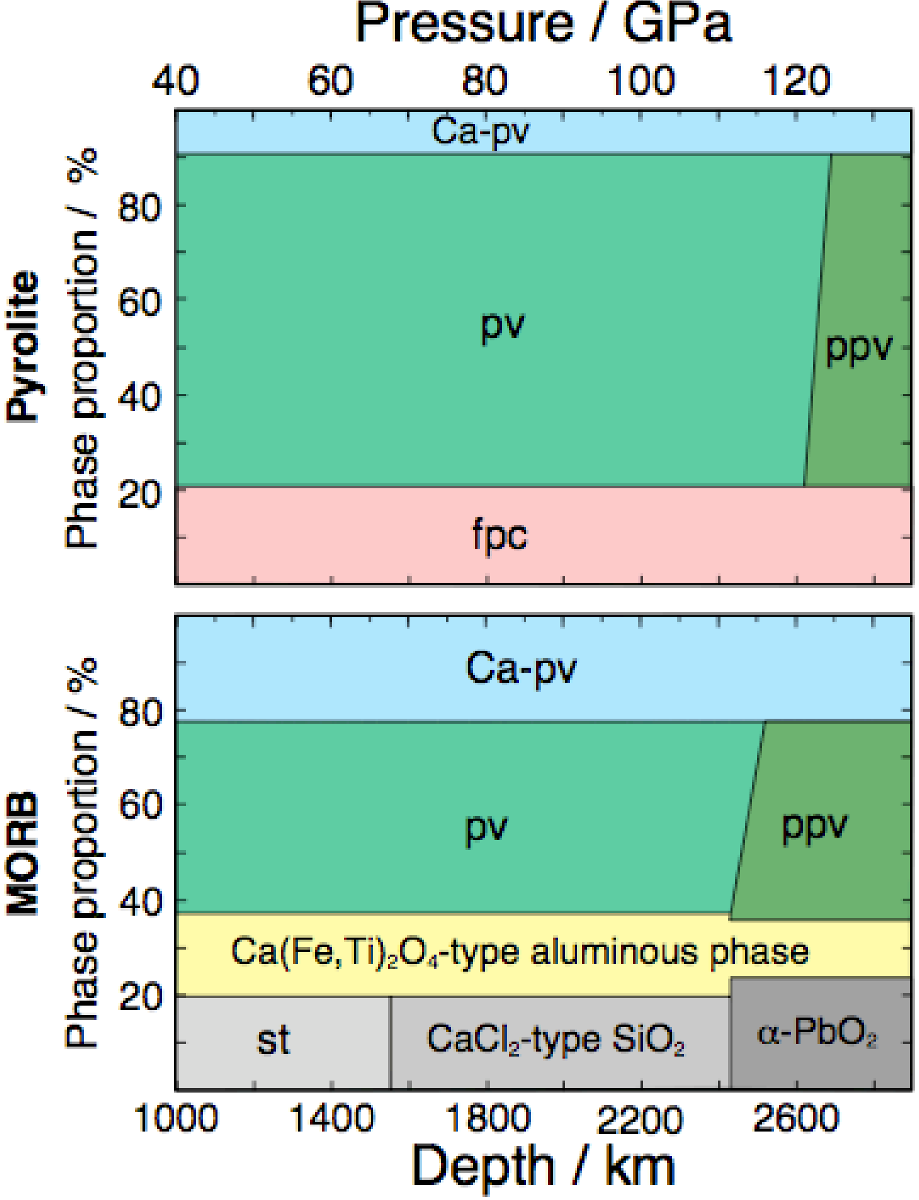

Perovskite to Post-perovskite

Ab initio modelling of PPV

(Oganov and Ono, 2004; Stackhouse et al, 2005; Wookey et al, 2005b; Tsuchya et al, 2004; 2005; Wentzcovich et al, 2006 …)

- Simulate PPV at a range of near-CMB P-T
- Observe strong (exothermic) temperature dependence in phase-boundary depth

A lower mantle temperature probe.

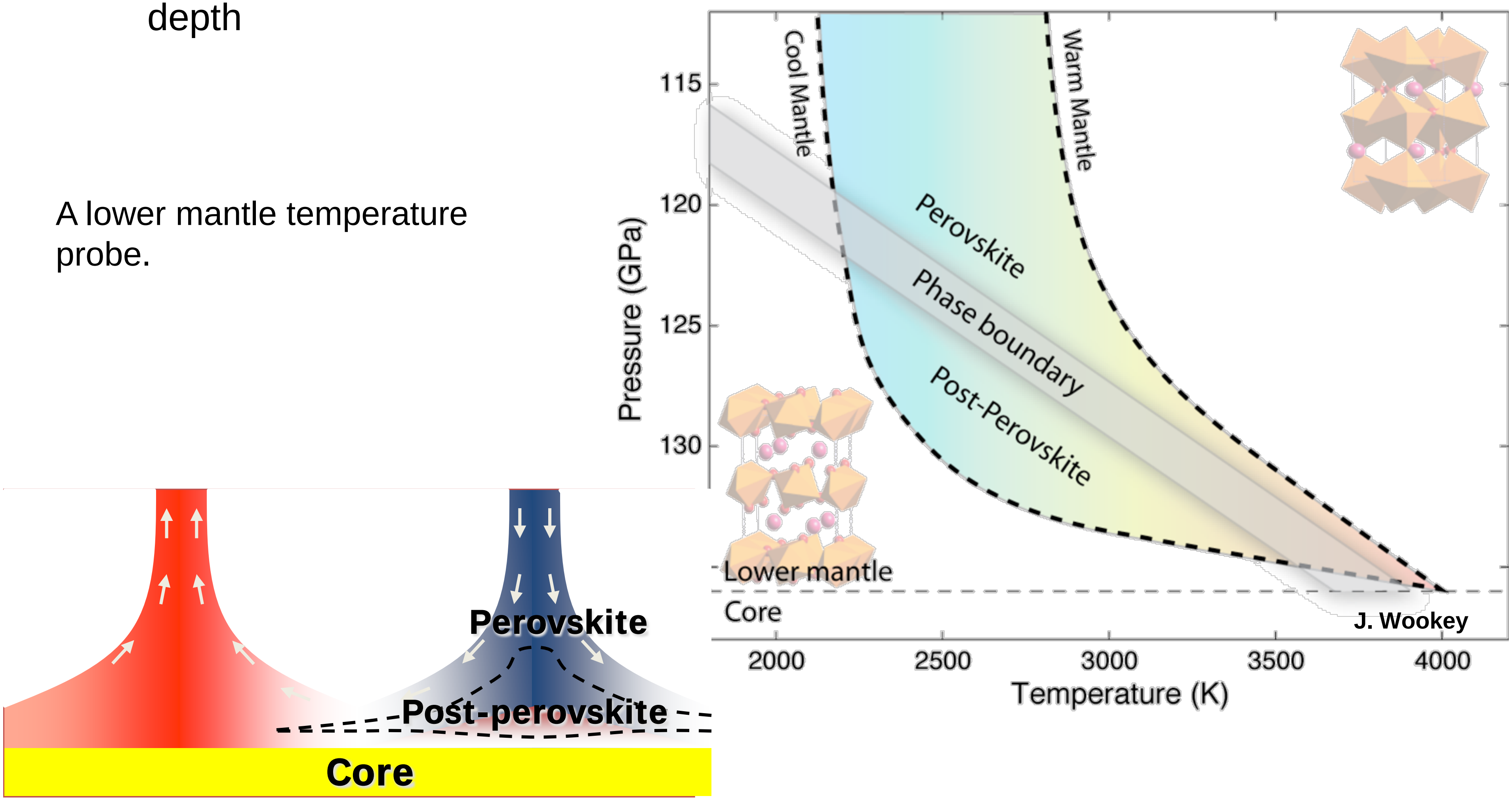

The elasticity of the lower mantle

- Perovskite
- Orthorhombic symmetr
- Moderately anisotropic comparable magnitude and symmetry betweer authors.

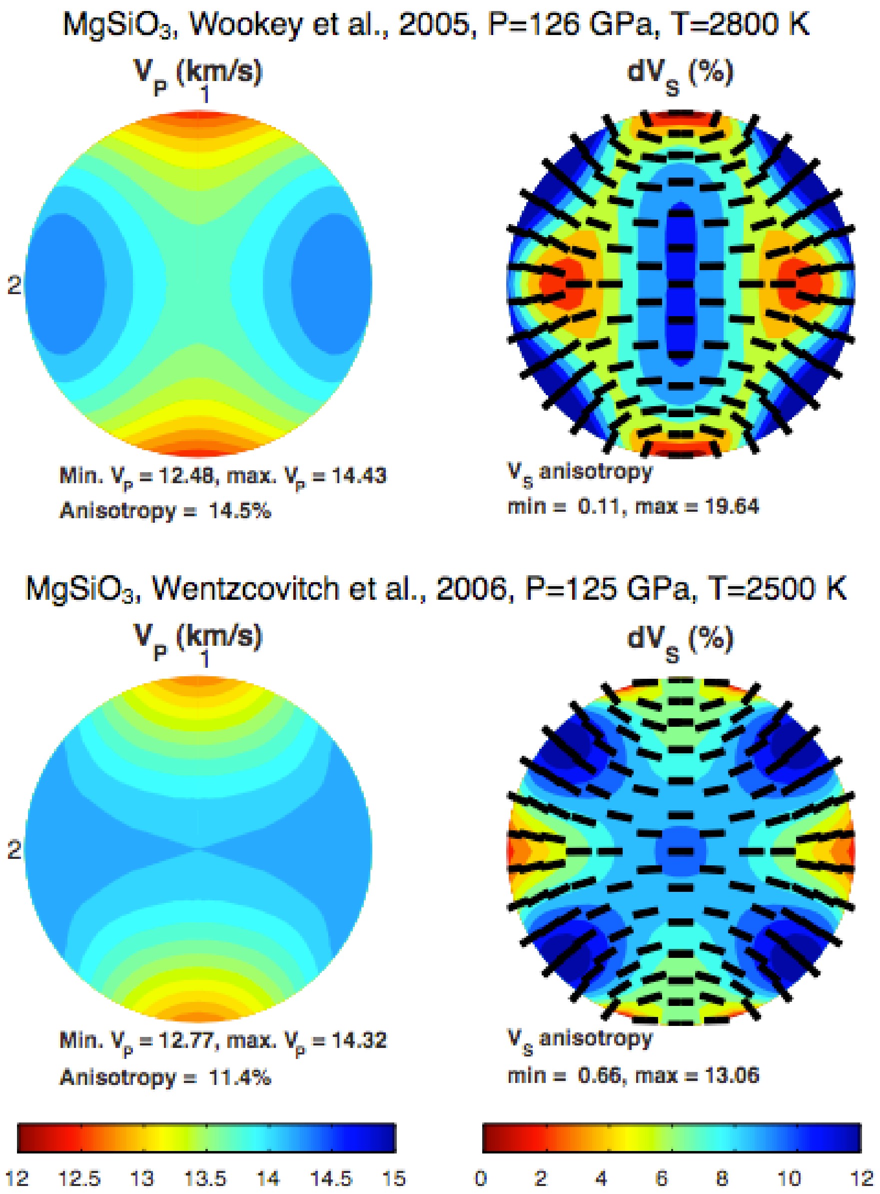
$MgSiO_3$, Wookey et al., 2005, P=126 GPa, T=2800 K

V_P (km/s)

dV_S (%)

Min. V_p = 12.48, max. V_p = 14.43
Anisotropy = 14.5%

V_S anisotropy
min = 0.11, max = 19.64

$MgSiO_3$, Wentzcovitch et al., 2006, P=125 GPa, T=2500 K

V_P (km/s)

dV_S (%)

Min. V_p = 12.77, max. V_p = 14.32
Anisotropy = 11.4%

V_S anisotropy
min = 0.66, max = 13.06

The elasticity of the lower mantle

- Postperovskite
- Orthorhombic symmetry
- Moderate to high amounts of anisotropy; more disagreement between authors.

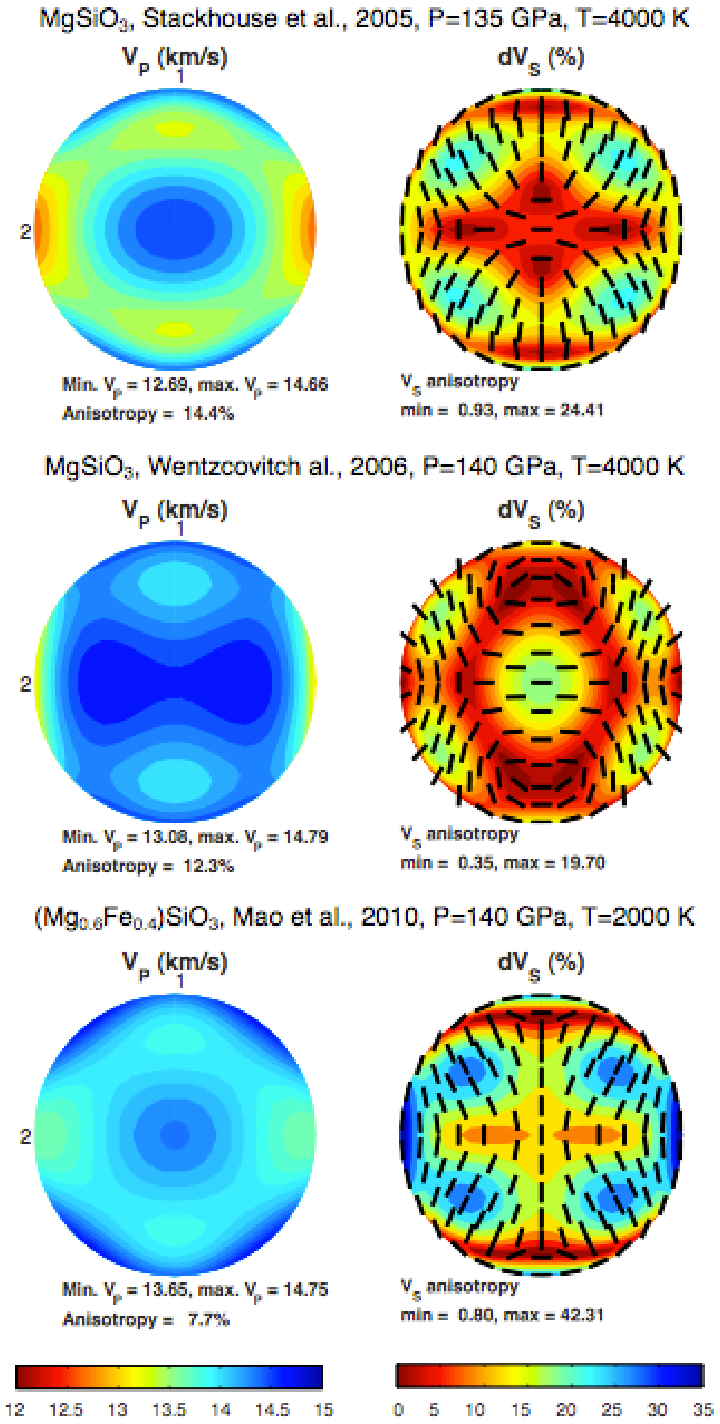

Lattice preferred orientation

- Deformation accommodated by many mechanisms.
- Dislocation more effective than diffusion in generating anisotropy.
- Temperature, grain size, strain rate, strain history, pressure, fluids
- Polymineralic effects?
- Inherited textures?
- Need to know slip systems.

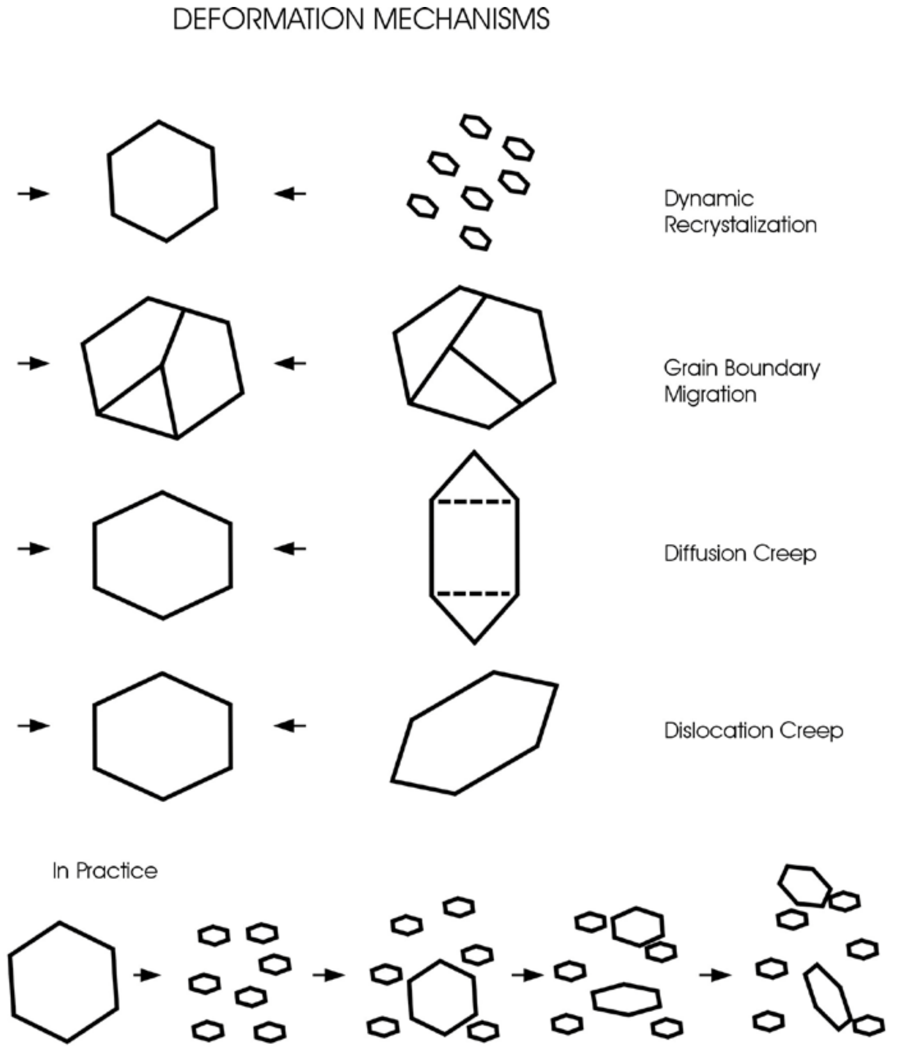

Controlling Factors:
temperature, grain size, stress-strain rate, pressure, fluids.

Postperovskite slip systems

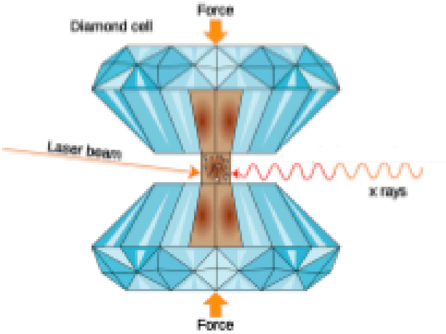

In situ deformation in the diamond anvil cell (to CMB pressure)

Peierls-Nabarro modelling using density functional theory

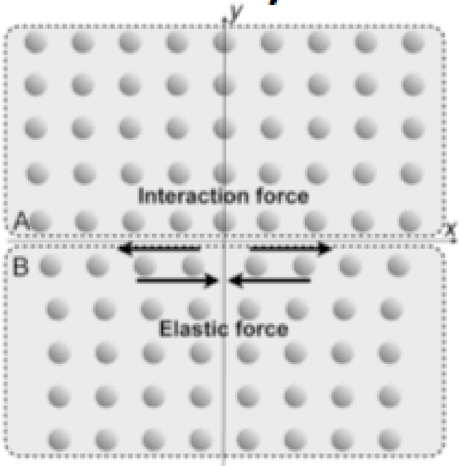

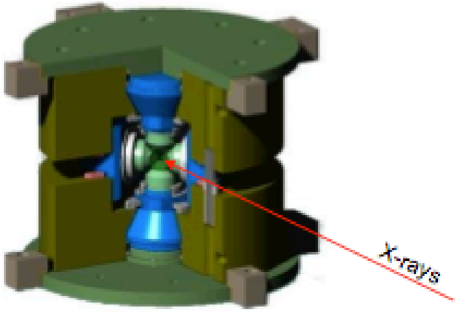

Large volume deformation experiments on analogues (elevated P & T)

$MgSiO_3$	(100) or (001)	(010)	-
$CaIrO_3$	(010)	(010)	(010)

Other anisotropy mechanisms

- **Shape-preferred orientation (SPO)**
  - Layering of contrasting materials (Backus 1962)
  - Alignment of inclusions (e.g., Kendall and Silver, 1996)
  - Candidate inclusion materials include basaltic melt (Hirose et al, 1999), or intrusions of core material
  - Combination of SPO and LPO (e.g., Holtzman and Kendall, 2010)

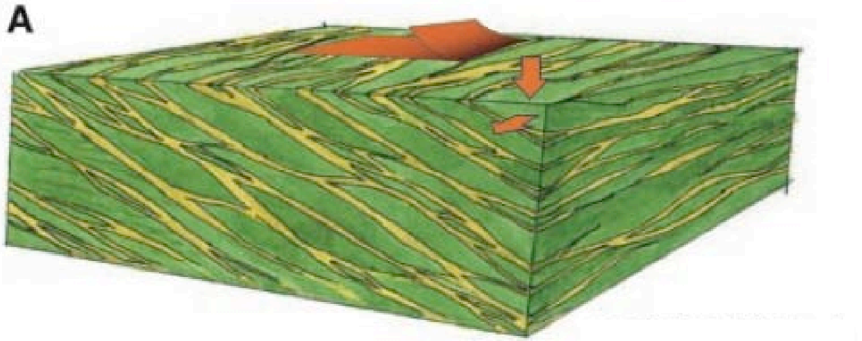

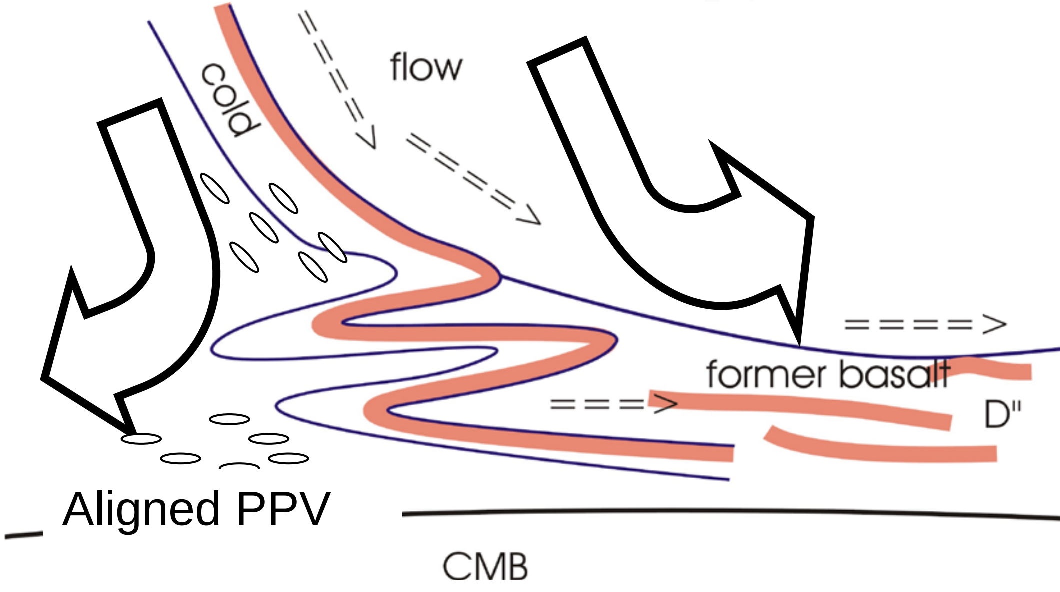

A seismic probe of lower-mantle anisotropy

- Shear-wave splitting

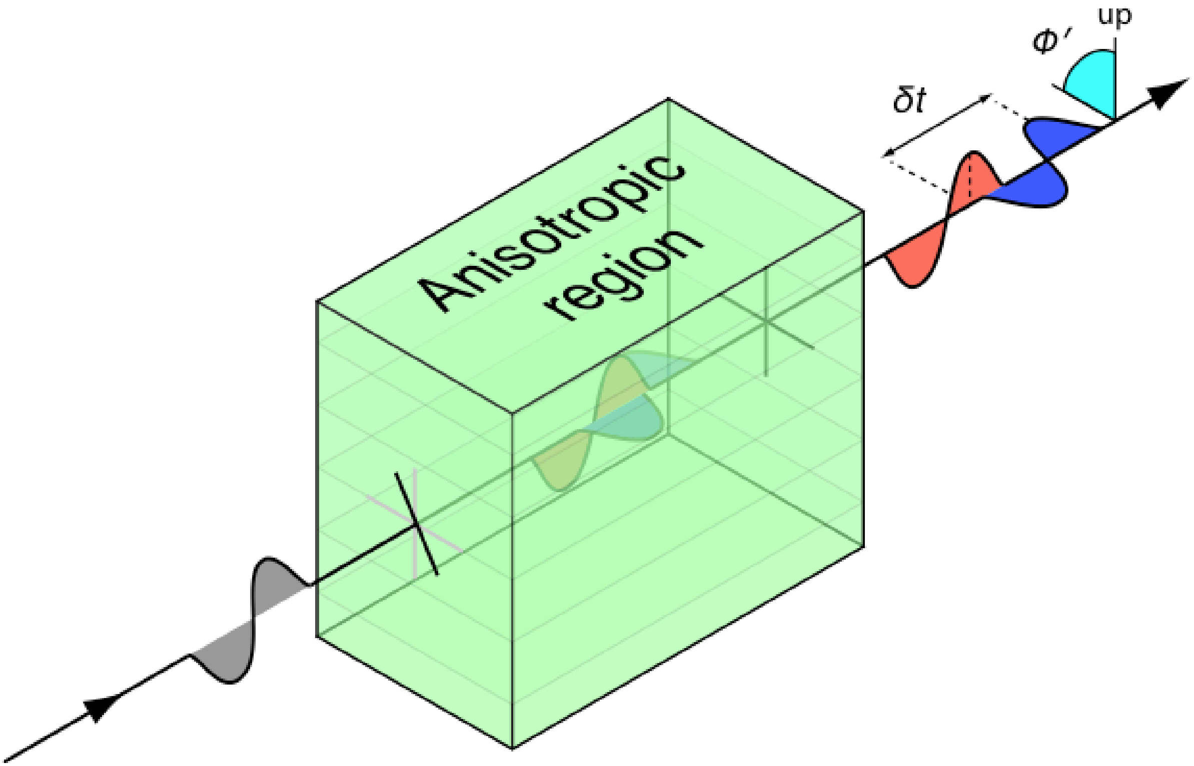

Lower mantle anisotropy

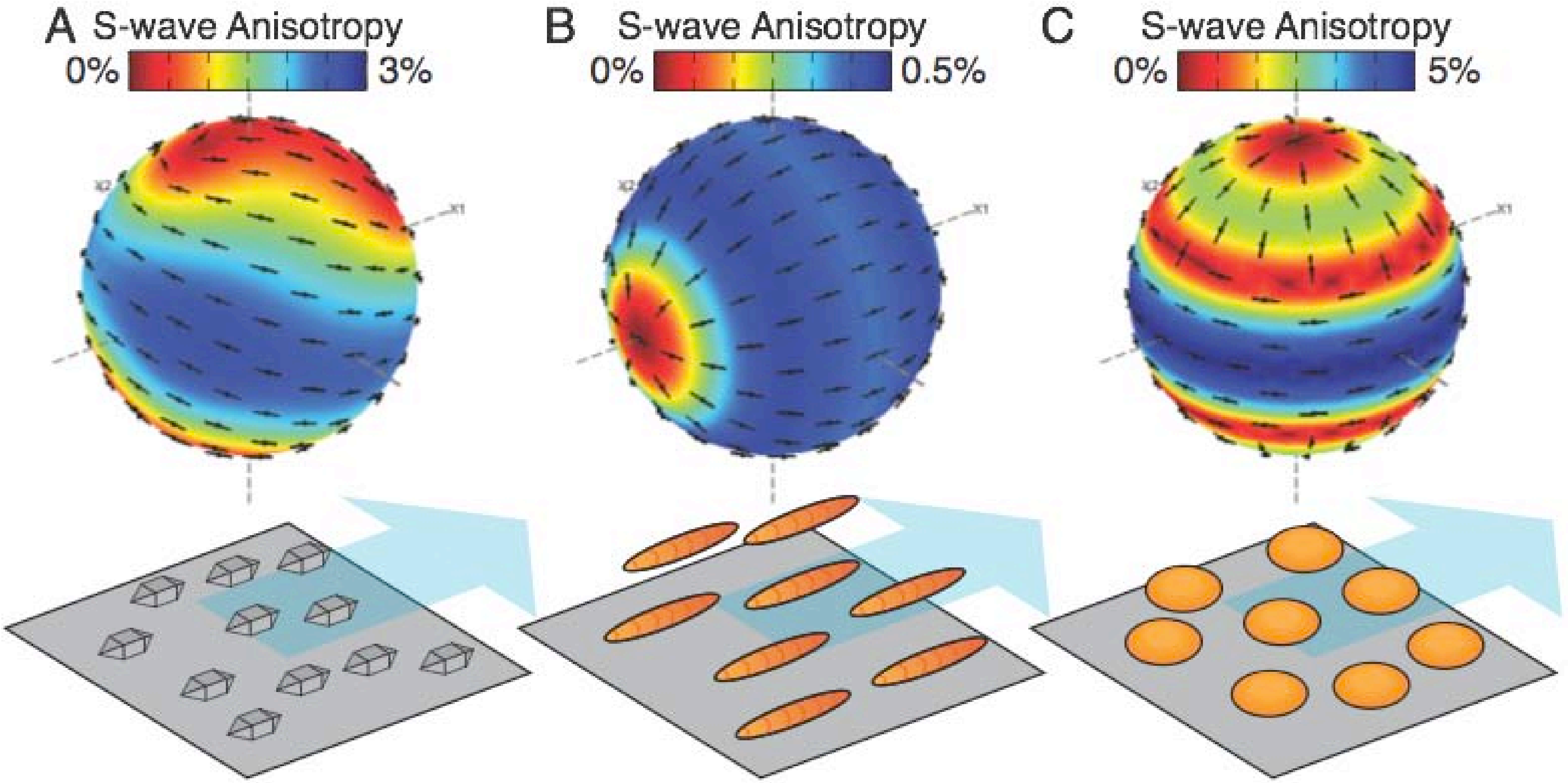

VTI anisotropy

- Simple example is layering …

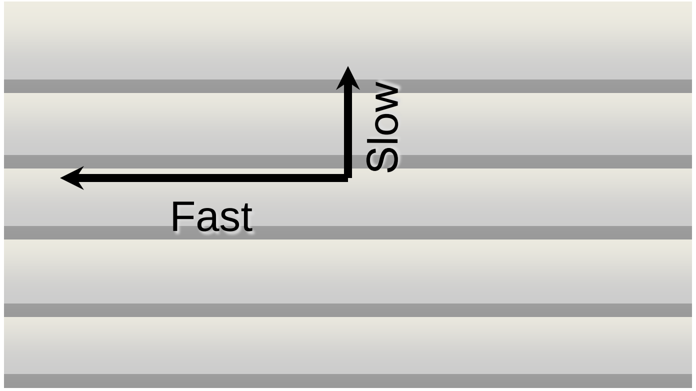

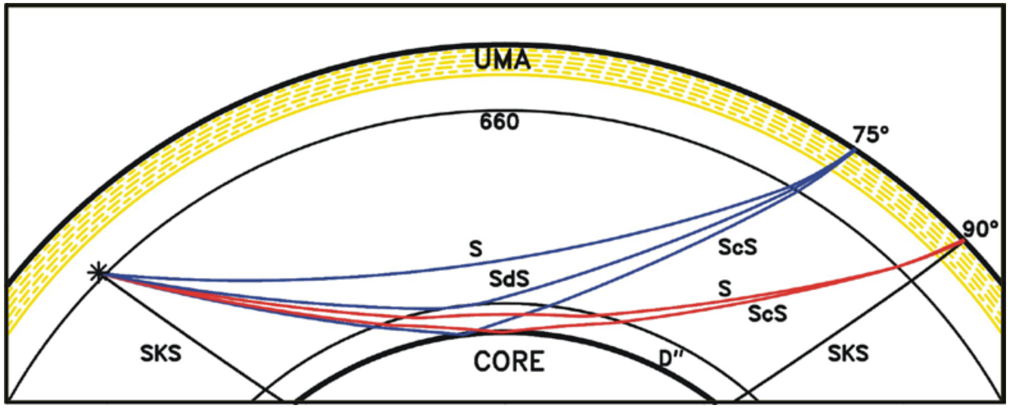

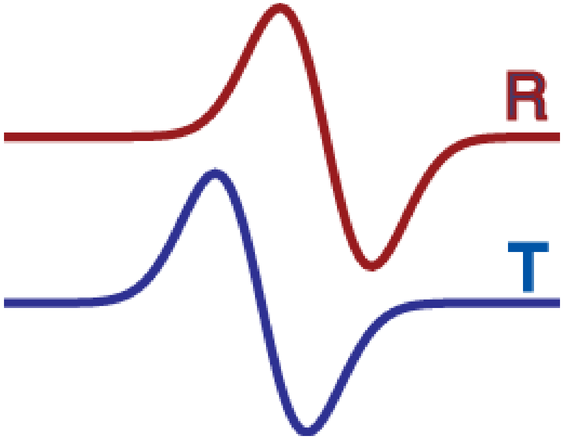

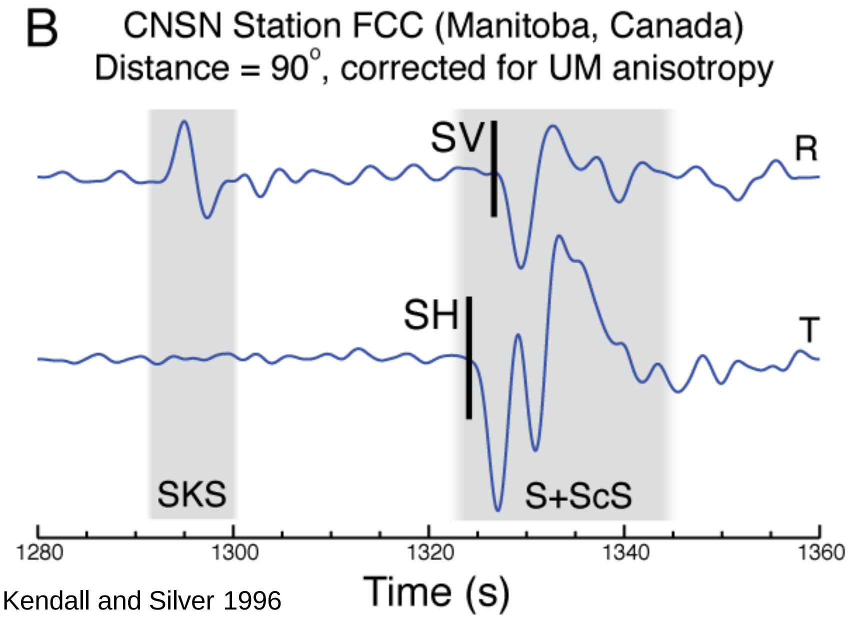

Kendall and Silver 1996

Global map of VTI anisotropy: clear regional variations

Tomography 75 km above CMB

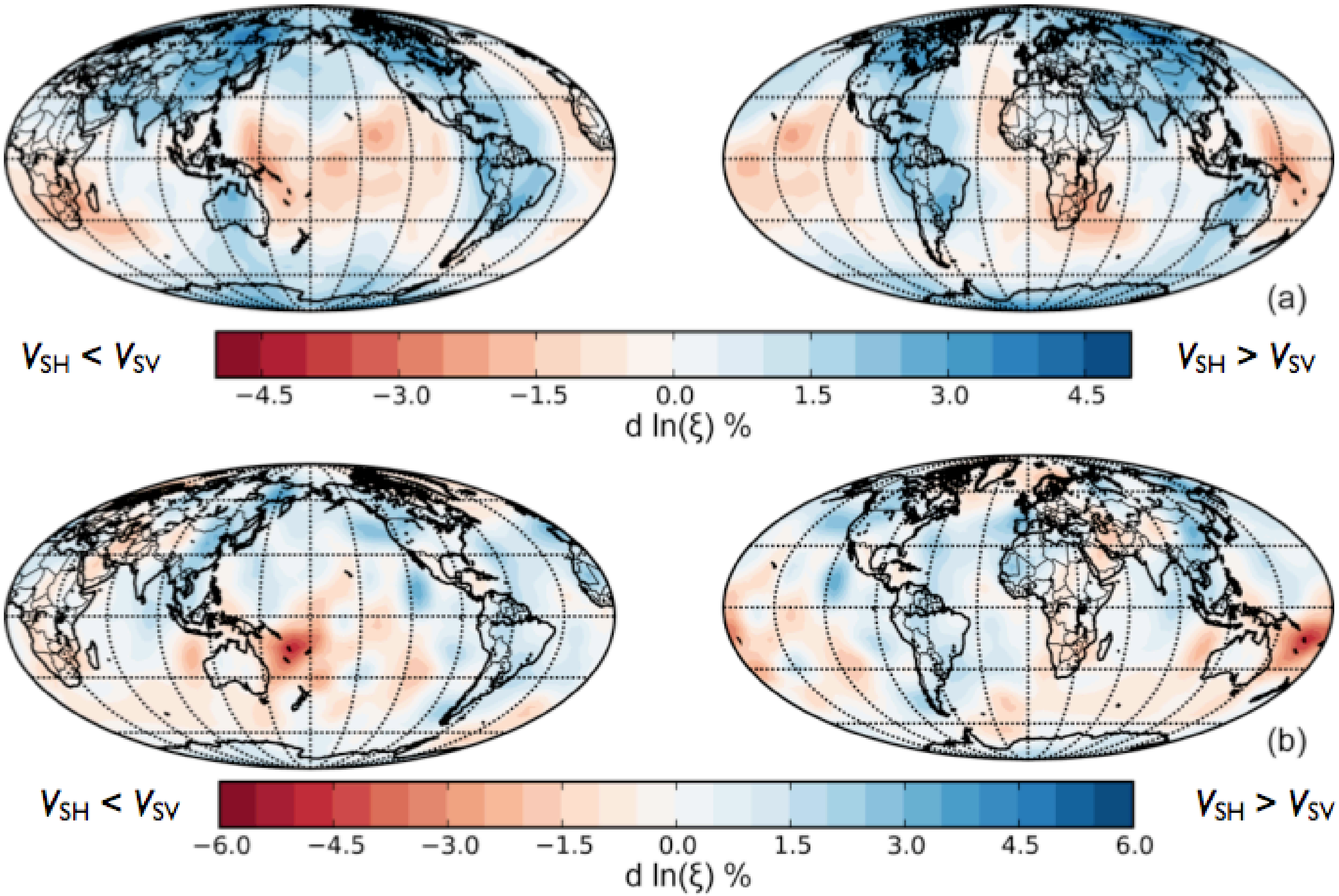

(a) Panning and Romanowicz 2006 *Geophys. J. Int.* 167:361-379
(b) Kustowski *et al.* 2008 *J. Geophys. Res.* 113: B06306

Isolating more general forms of anisotropy (non-VTI)

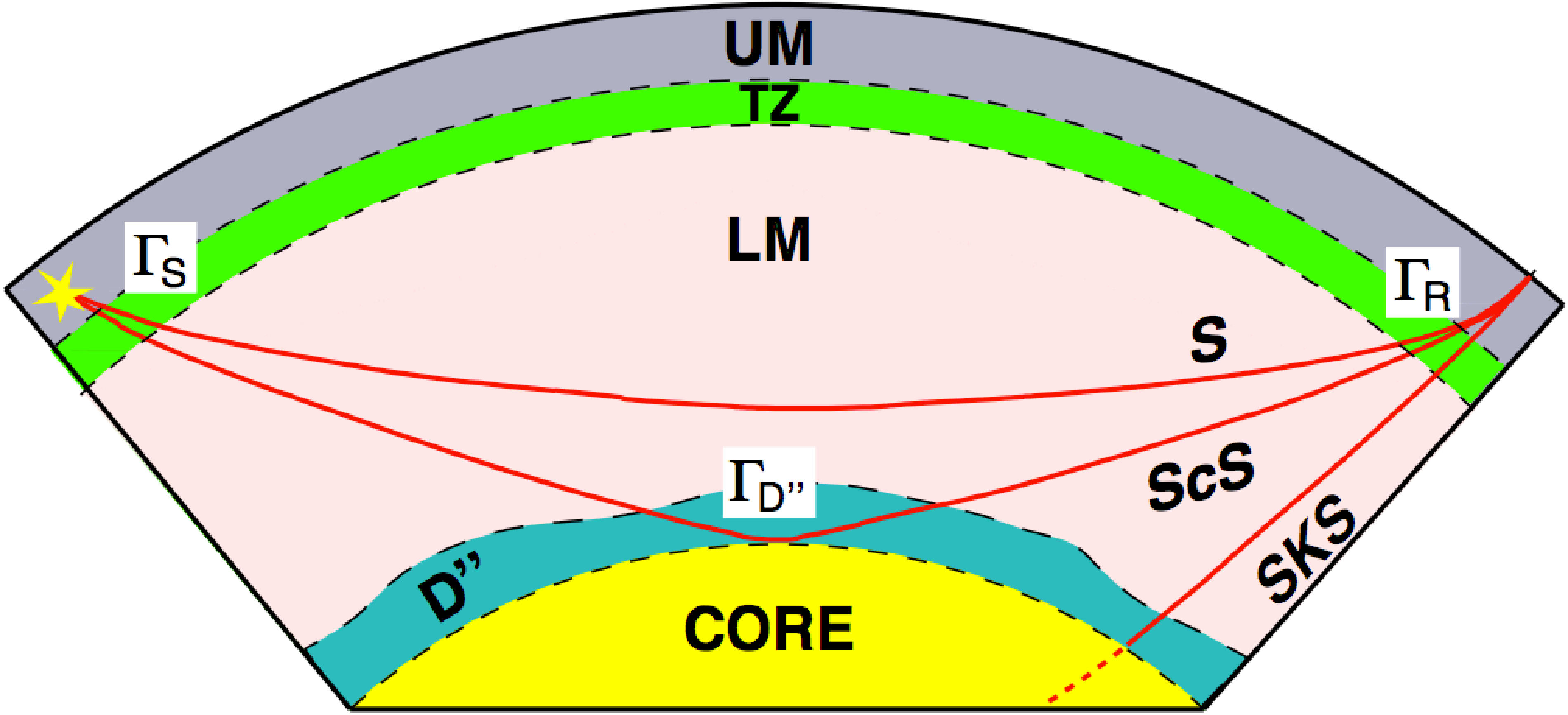

Source side shear-wave splitting analysis (e.g., Wookey et al., 2005; Wookey and Kendall. 2008; Nowacki et al., 2010; 2013)

University of BRISTOL

Crossing paths in the lowermost mantle:

- Much better resolution of anisotropy (2 vectors of fast shear-wave polarisation to define the symmetry plane)
- Potential to distinguish TI from orthorhombic medium

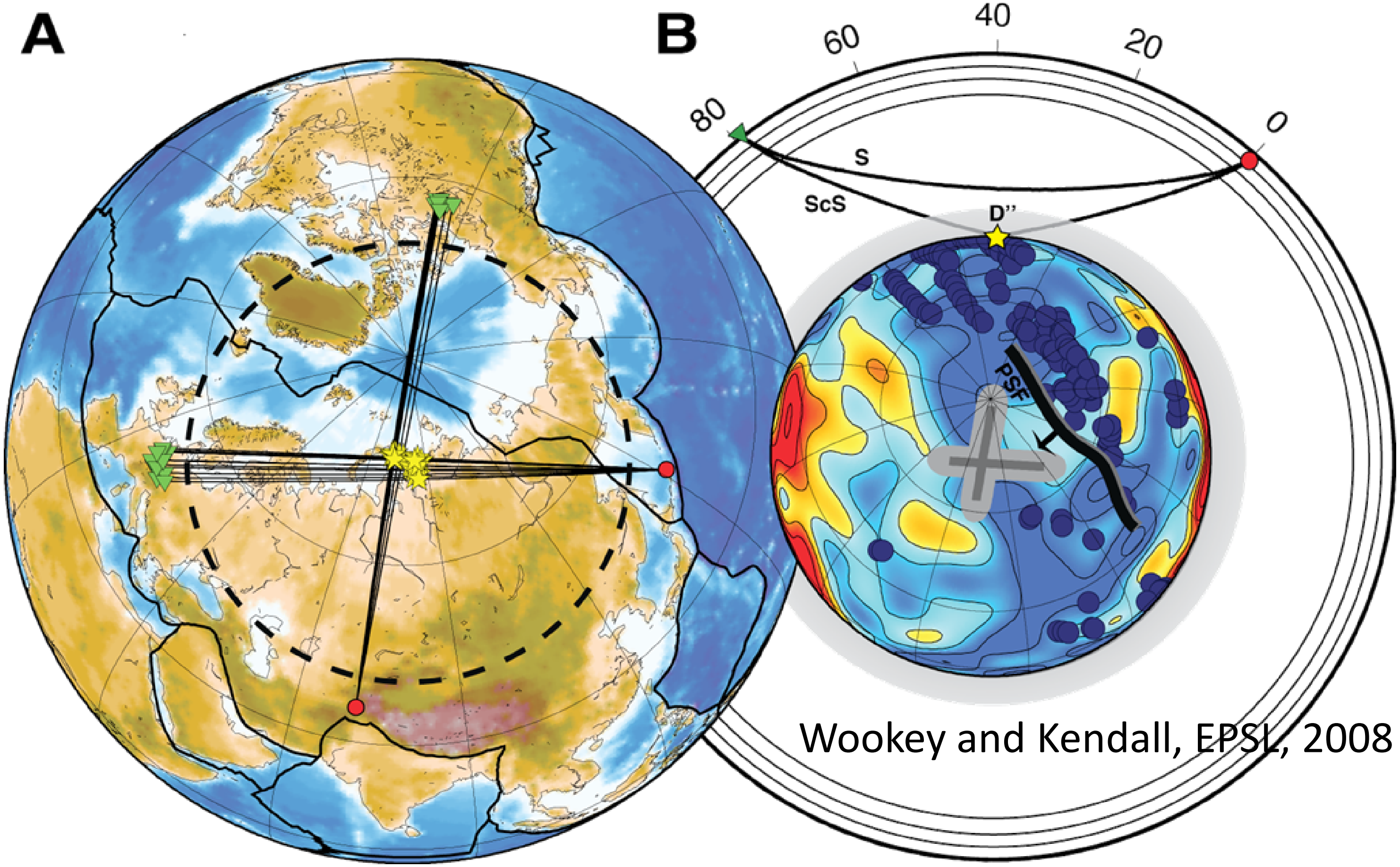

Wookey and Kendall, EPSL, 2008

University of BRISTOL

NWK methodology

Rigorous data selection and quality control:

- Simple and well characterised receiver anisotropy.
- Use data from similar azimuths for both S and SKS.
- High-quality measurements, low error, clear signal and anisotropy.
- Inferred source polarisation must agree with CMT solution for the earthquake.

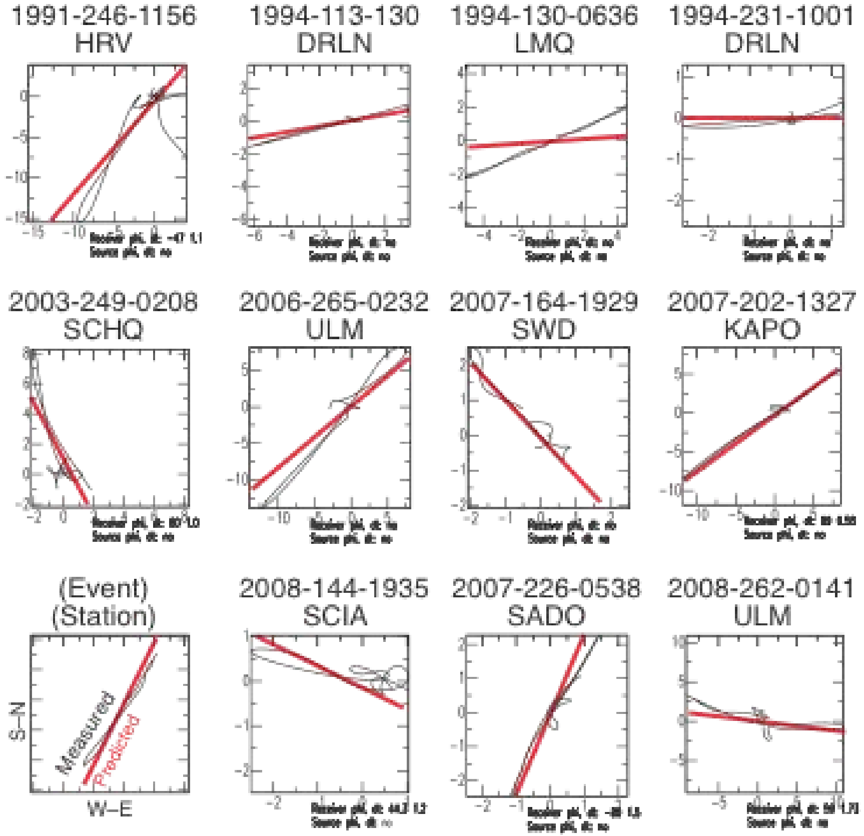

Nowacki, Wookey and Kendall, Nature 2010

Anisotropy beneath the Americas

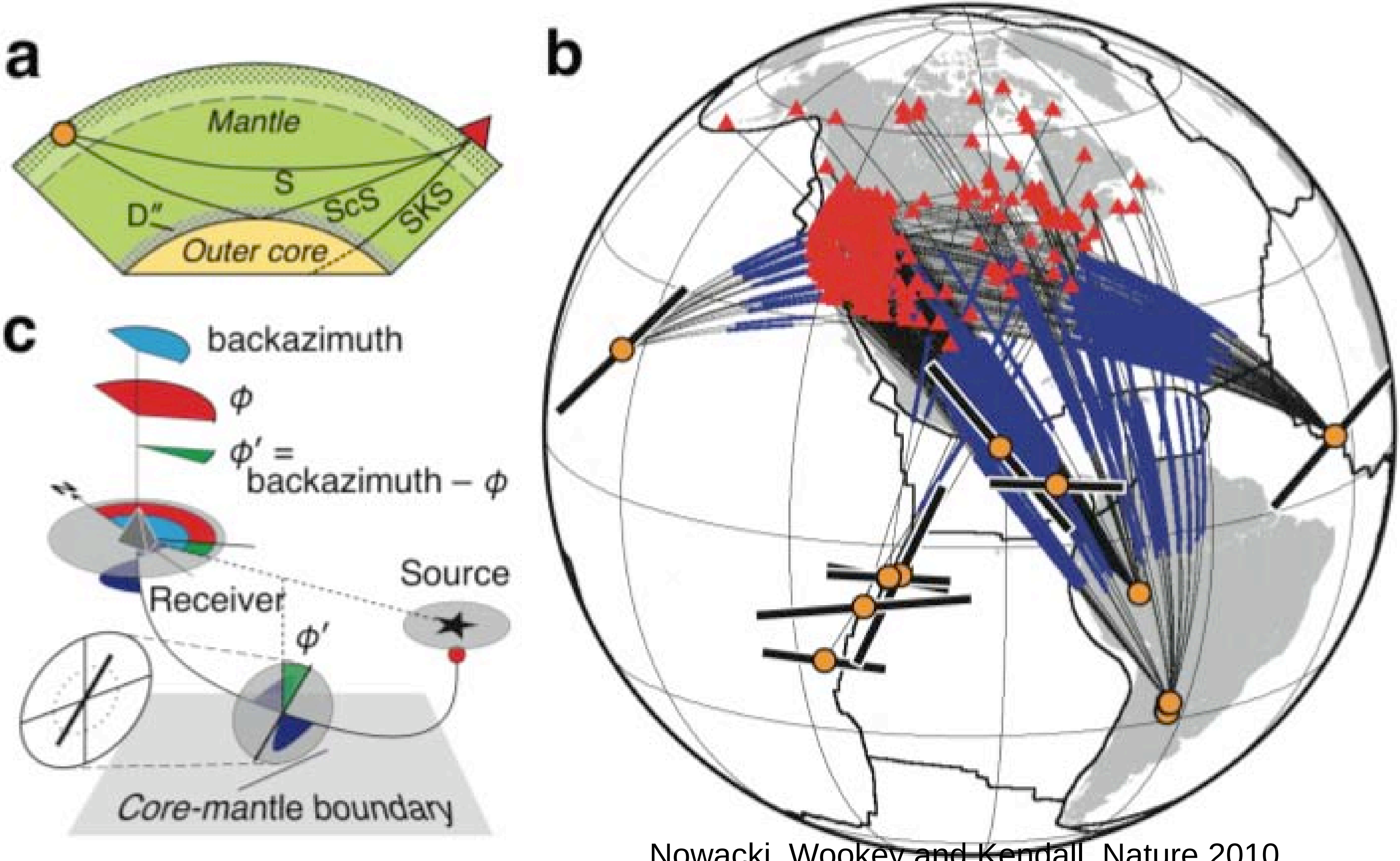

Nowacki, Wookey and Kendall, Nature 2010

Anisotropy beneath the Americas: best fitting TTI model

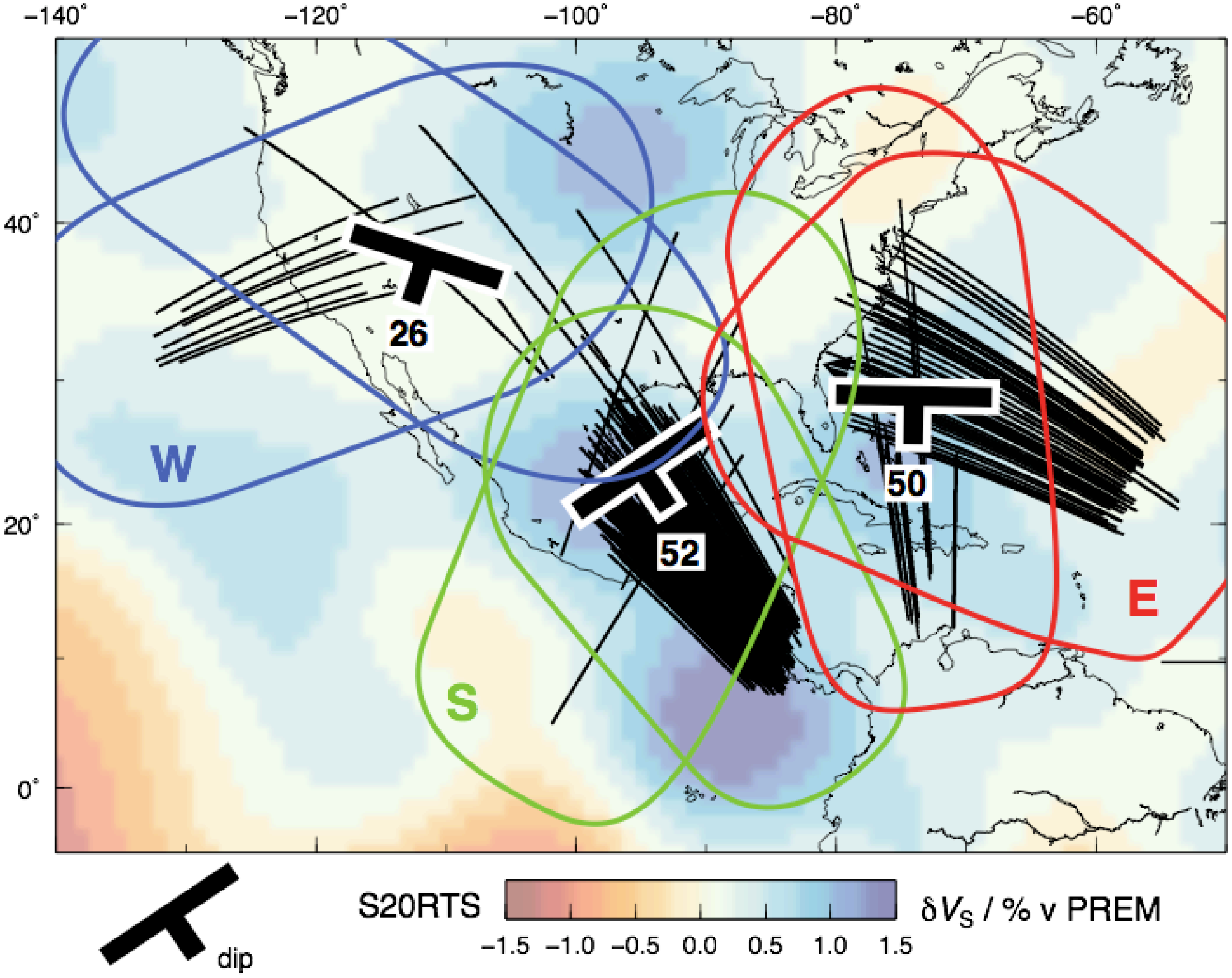

Nowacki, Wookey and Kendall, 2010

The current picture

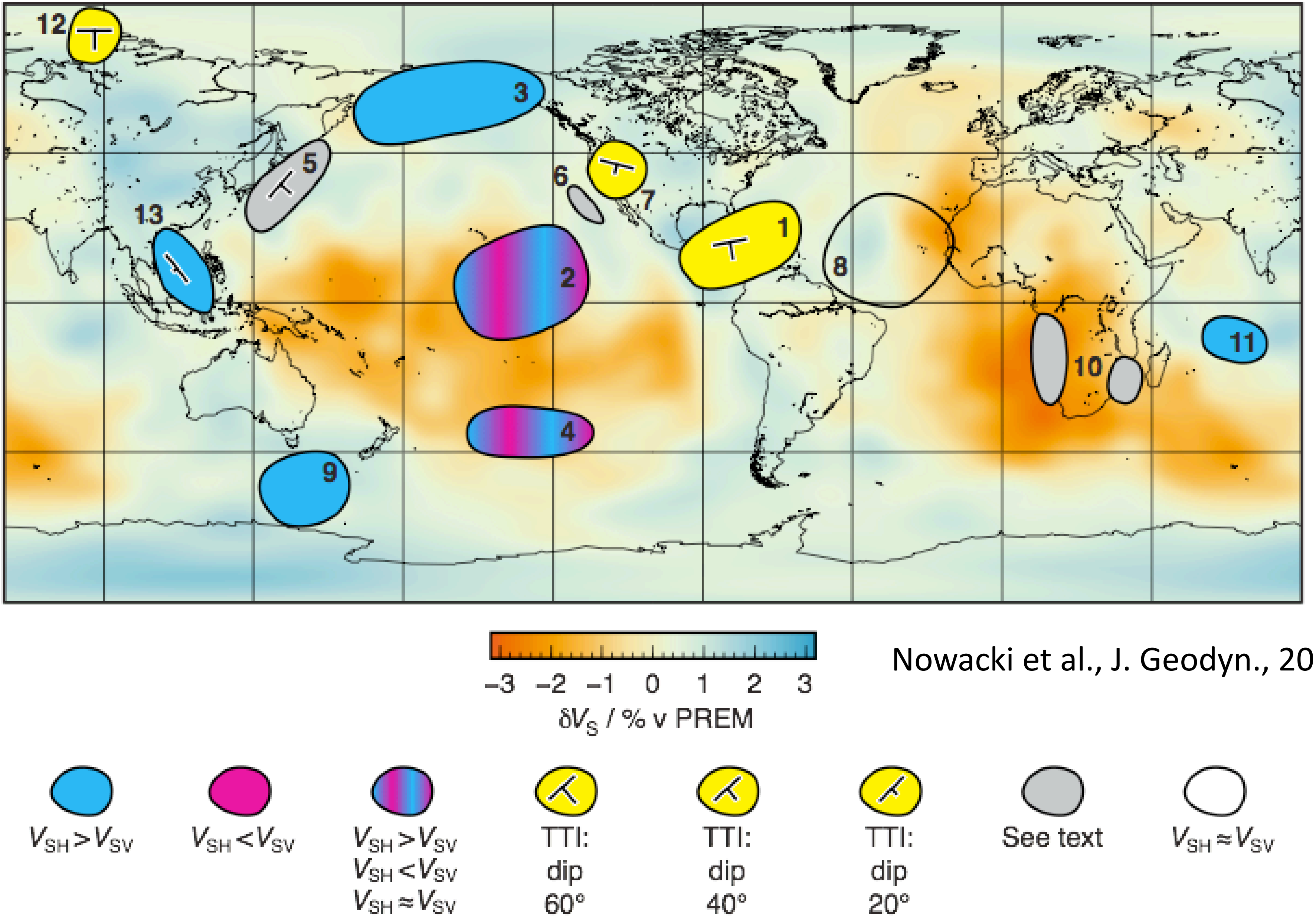

Nowacki et al., J. Geodyn., 2011

… next steps

- We test ppv as a causative mechanism for D” anisotropy.
- Use current best knowledge of ppv elasticity and slip systems
- Use state of the art models of mantle flow, which incorporate chemistry (e.g., Simmons et al., 2009)
- Ideally consider strain history in 3D
- Ideally impose no restriction on style of anisotropy

See: Walker et al., G3, 2011; Wenk et al., EPSL, 2011; Nowacki et al., GJI, 2013

University of BRISTOL

Linking flow, mineralogy and seismic observations

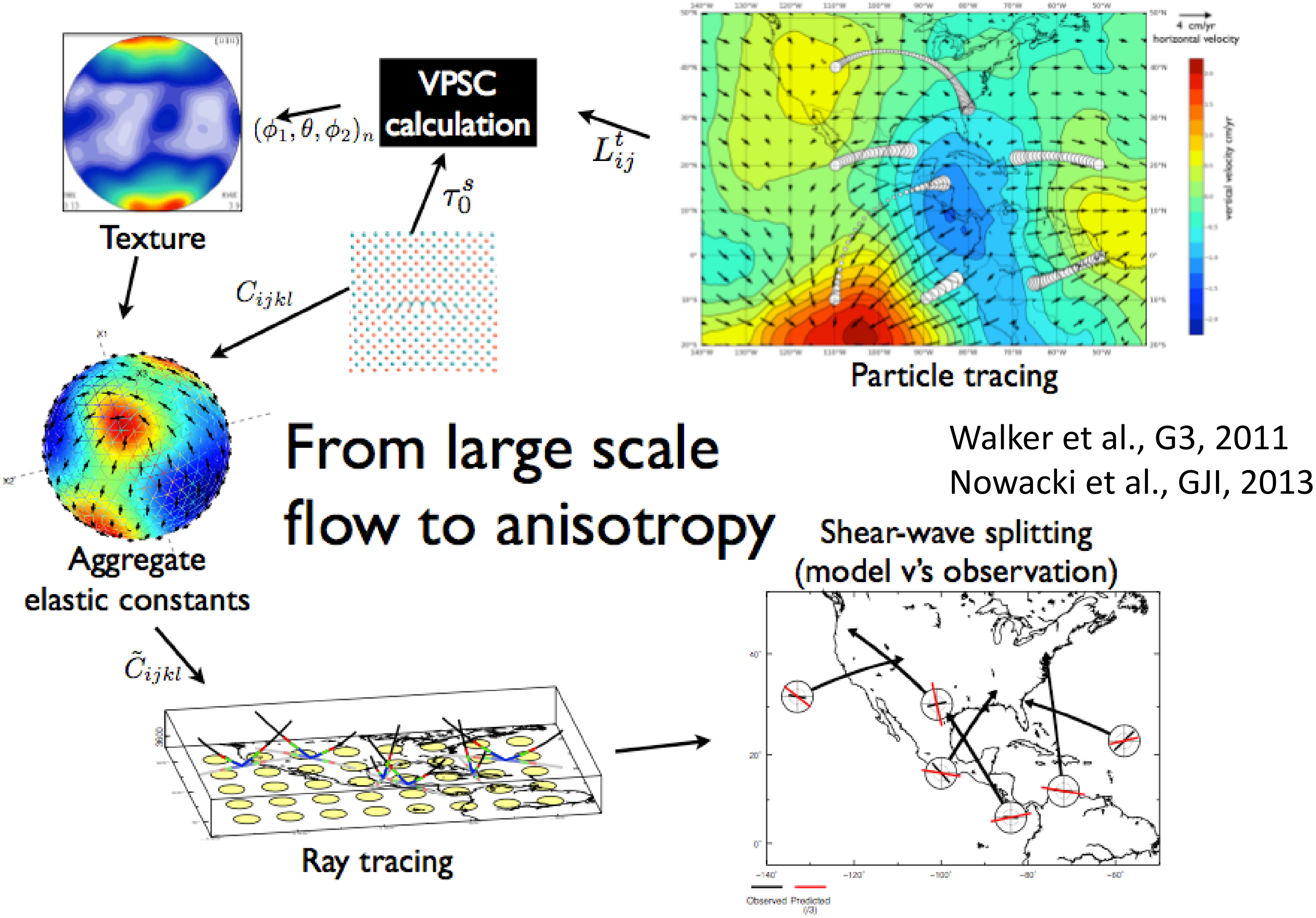

Texture

$(\phi_1, \theta, \phi_2)_n$

VPSC calculation

L^t_{ij}

τ^s_0

C_{ijkl}

Particle tracing

Aggregate elastic constants

$\tilde{C}_{ijkl}$

Ray tracing

Shear-wave splitting (model v's observation)

From large scale flow to anisotropy

Walker et al., G3, 2011

Nowacki et al., GJI, 2013

See Walker et al., G3, 2011

Flow model from joint inversion

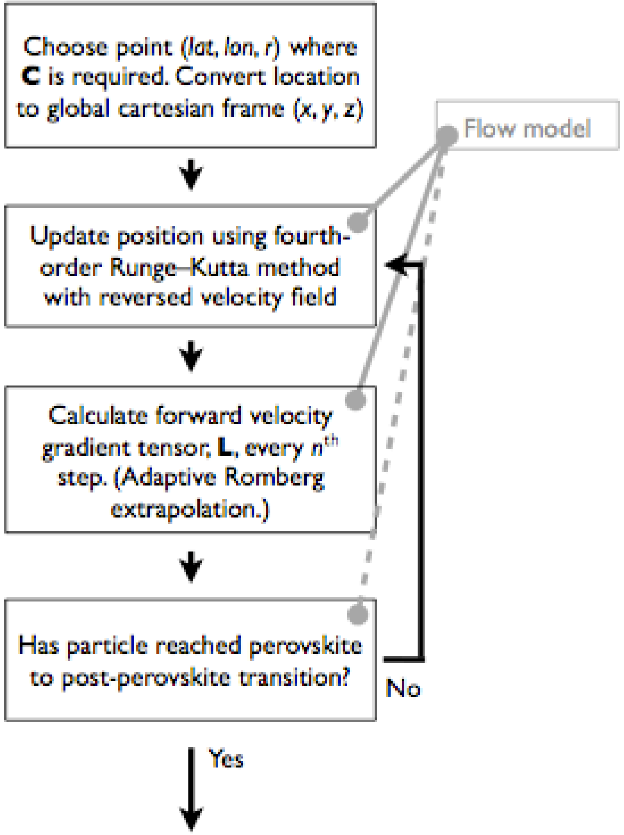

Choose point (*lat*, *lon*, *r*) where **C** is required. Convert location to global cartesian frame (*x*, *y*, *z*)

Update position using fourth-order Runge–Kutta method with reversed velocity field

Calculate forward velocity gradient tensor, **L**, every *n*th step. (Adaptive Romberg extrapolation.)

Has particle reached perovskite to post-perovskite transition?

$$(\mathbf{x}_{t_0}, \mathbf{x}_{t_1}, \ldots, \mathbf{x}_{t_N})$$

$$(\mathsf{L}_{t_0}, \mathsf{L}_{t_1}, \ldots, \mathsf{L}_{t_N})$$

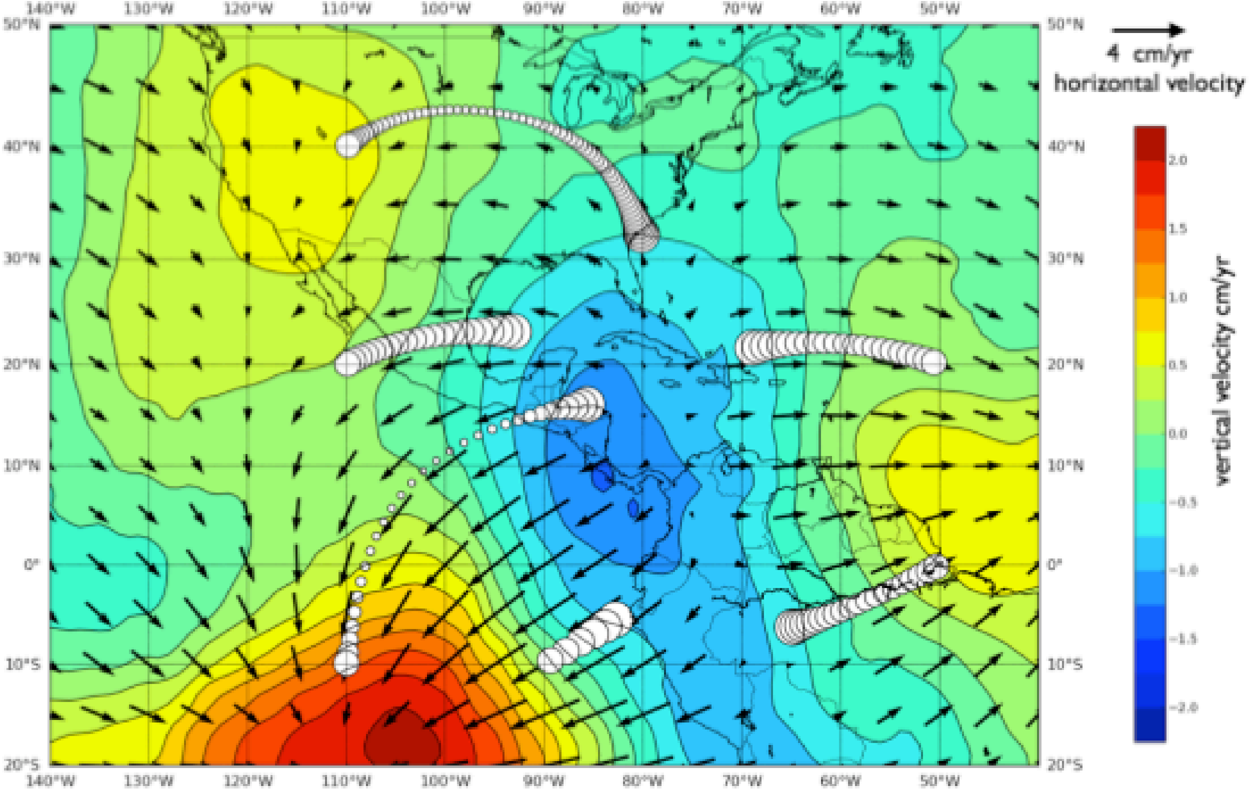

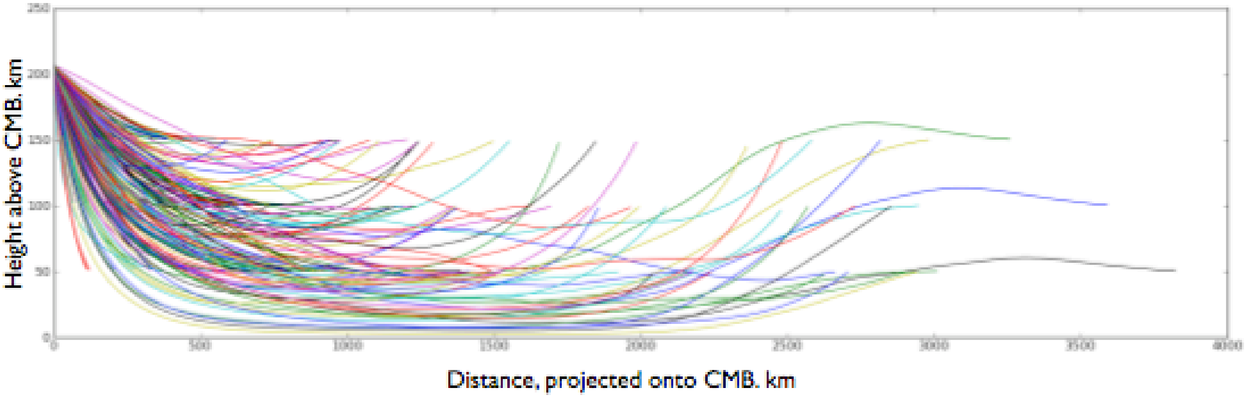

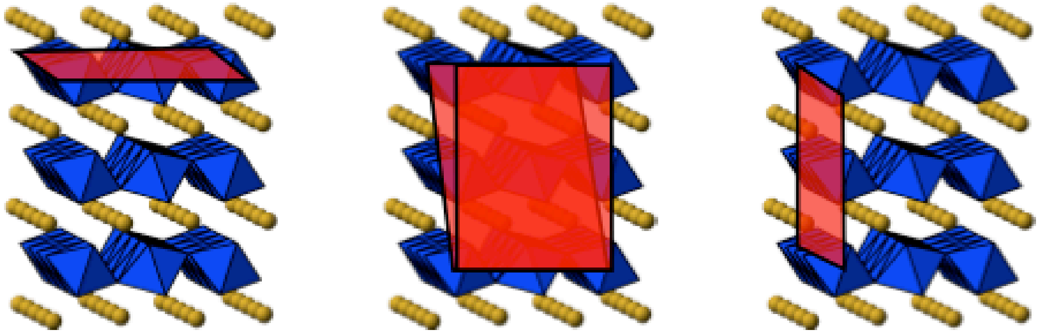

Slip system	PN: (010)[a]	{110}/(100)[b]	(001)[c]
[100](001)	2.6	10	1
[010](001)	4.1	10	1
[001](010)	1.0	∞	∞
[001](100)	5.4	2	10
[010](100)	5.2	1	10
[001]{110}	2.9	4	10
<110>(001)	4.1	10	2
[100]{011}	6.8	∞	∞
[100](010)	4.7	∞	∞
<110>{110}	8.8	1	10

[a] Metsue *et al.* 2009 *PEPI* 74:165-173

[b] Merkel *et al.* 2007 *Science* 316:1729-1732

[c] This work (*c.f.* Miyagi *et al.* 2010 *Science* 329:1636-1638)

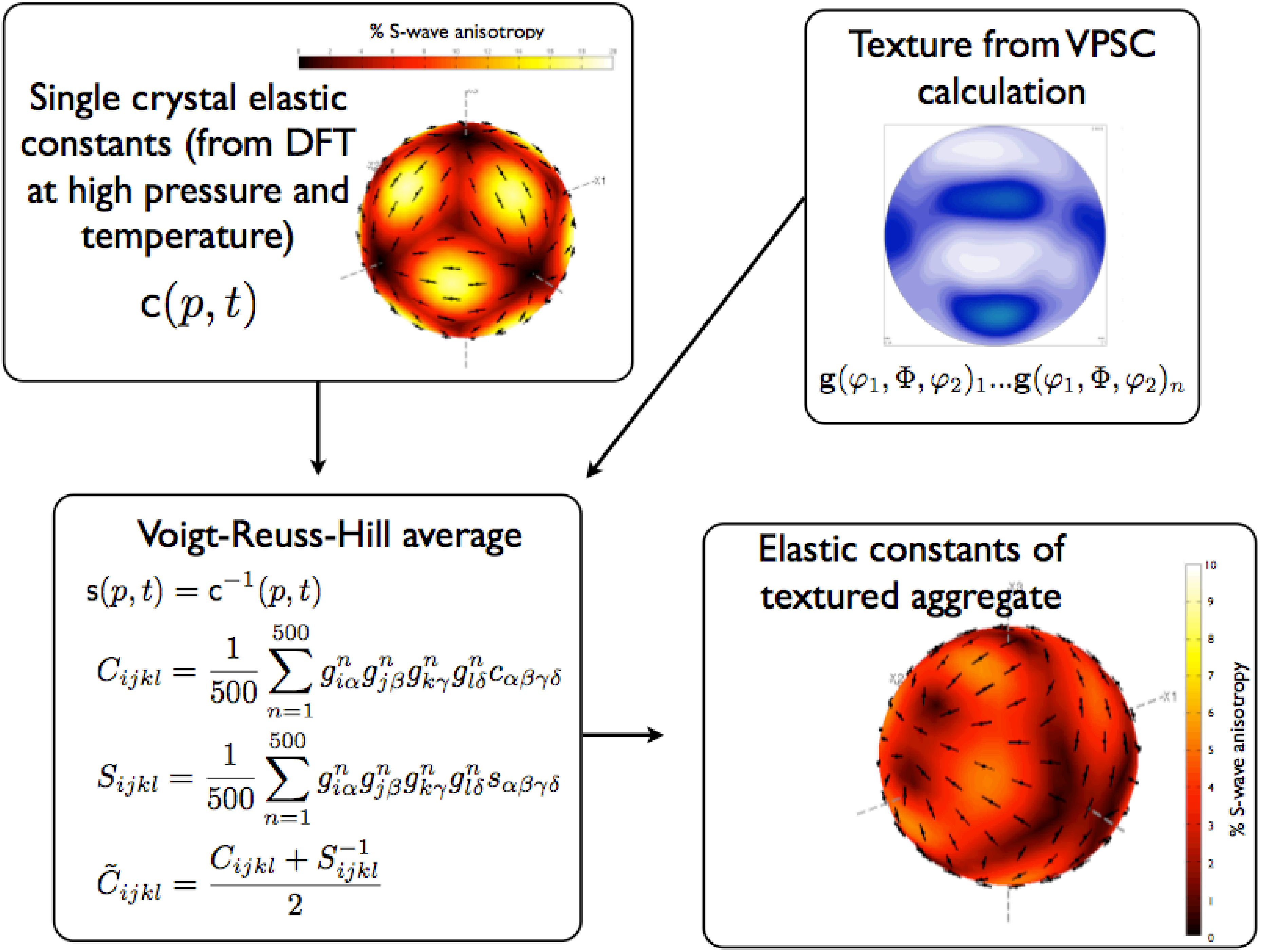

Single crystal elastic constants (from DFT at high pressure and temperature)

$$\mathsf{c}(p,t)$$

Texture from VPSC calculation

$$\mathbf{g}(\varphi_1,\Phi,\varphi_2)_1 \ldots \mathbf{g}(\varphi_1,\Phi,\varphi_2)_n$$

Voigt-Reuss-Hill average

$$\mathsf{s}(p,t) = \mathsf{c}^{-1}(p,t)$$

$$C_{ijkl} = \frac{1}{500}\sum_{n=1}^{500} g^n_{i\alpha} g^n_{j\beta} g^n_{k\gamma} g^n_{l\delta} c_{\alpha\beta\gamma\delta}$$

$$S_{ijkl} = \frac{1}{500}\sum_{n=1}^{500} g^n_{i\alpha} g^n_{j\beta} g^n_{k\gamma} g^n_{l\delta} s_{\alpha\beta\gamma\delta}$$

$$\tilde{C}_{ijkl} = \frac{C_{ijkl} + S^{-1}_{ijkl}}{2}$$

Elastic constants of textured aggregate

Generating Synthetic Seismograms

Ray-theoretical synthetic shear wave splitting for ray paths where we have observations

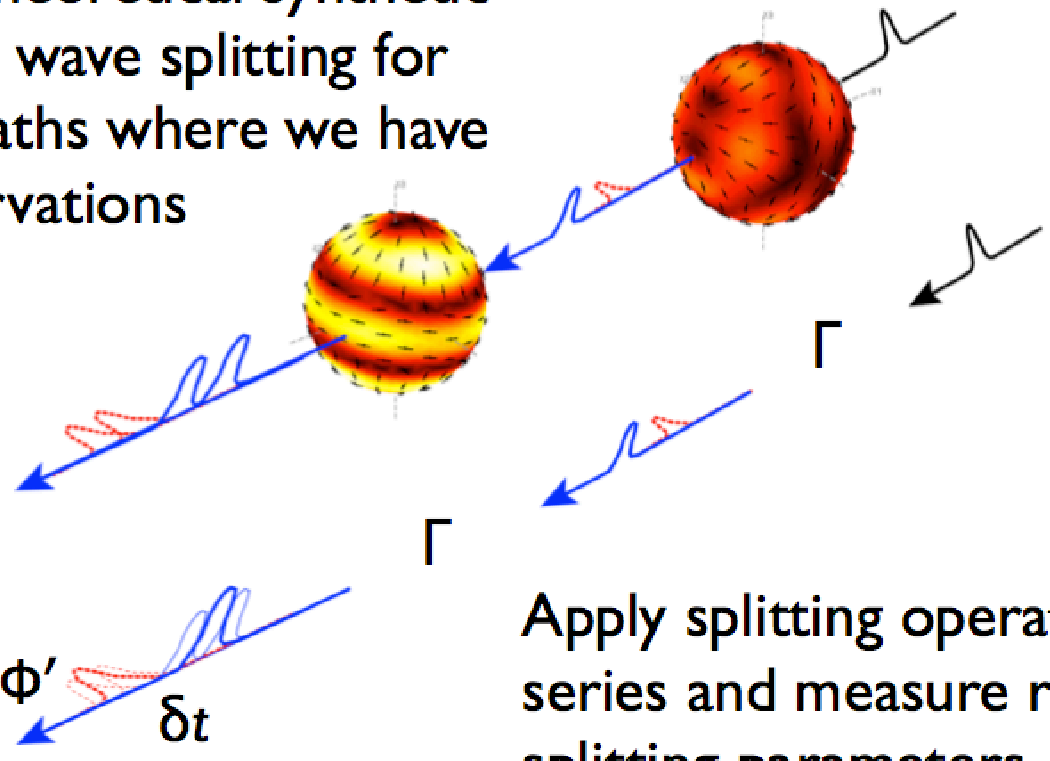

Apply splitting operators in series and measure resultant splitting parameters.

NB: δ*t* smaller than period of wave

University of BRISTOL

From observation to flow

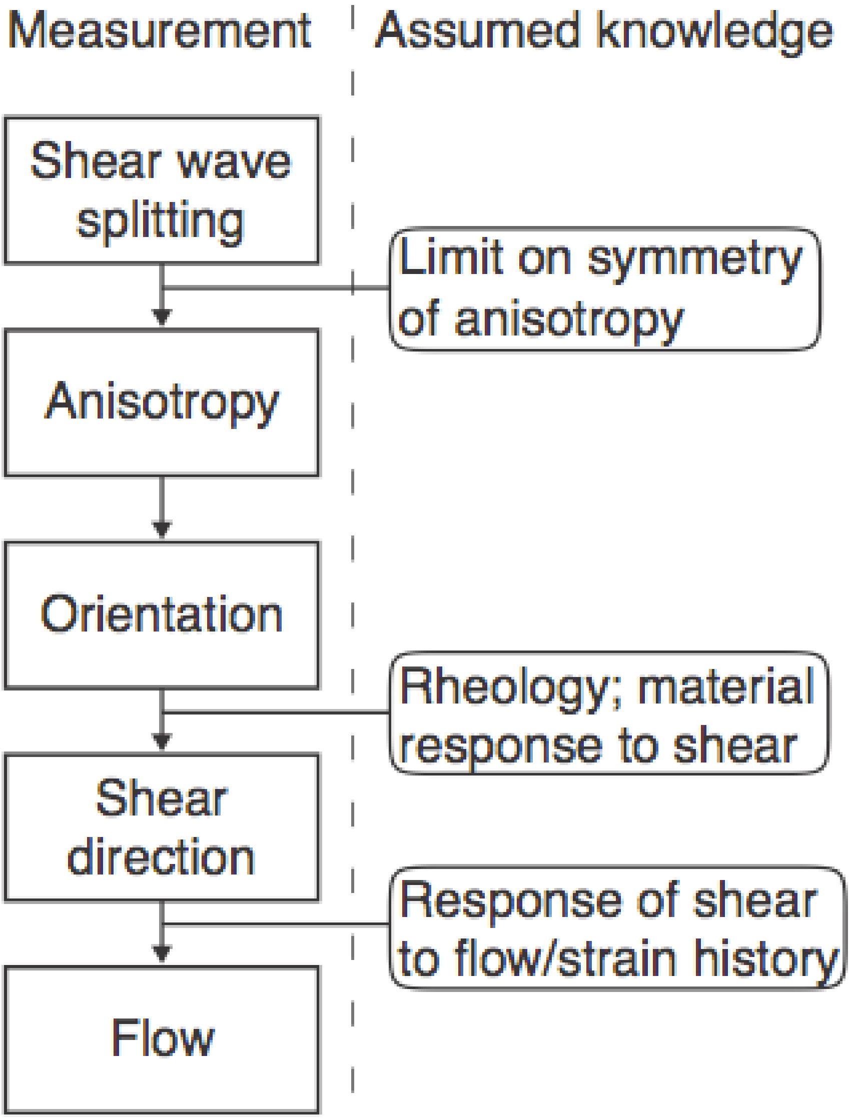

University of BRISTOL

Which slip system best fits the data? Ans = P010

- flow 200 km above the CMB; predicted by TX2008 (Simmons et al., 2009)
- VTI models: Panning et al. (2004; 2010); Kustowski et al. (2008)
- General form: Wookey et al. (2005; 2008); Nowacki et al. (2012)

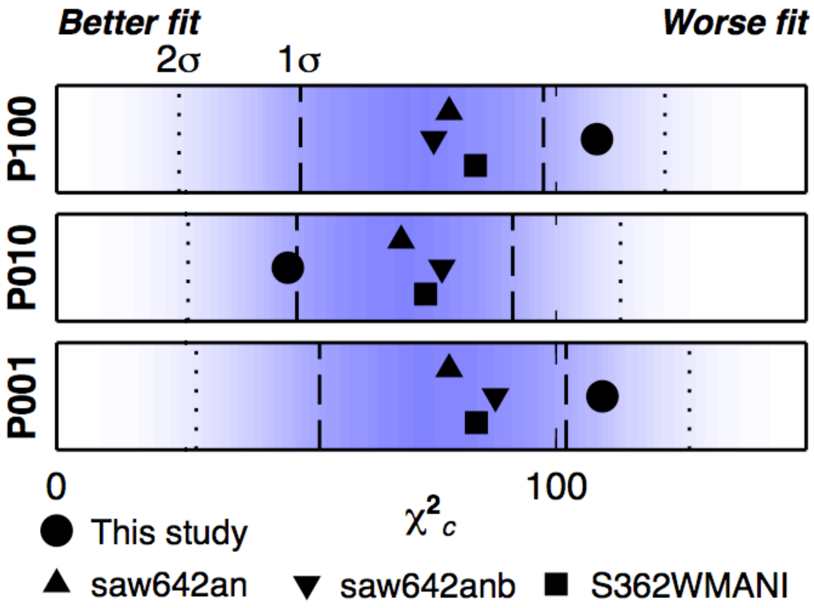

Nowacki et al., GJI, 2013

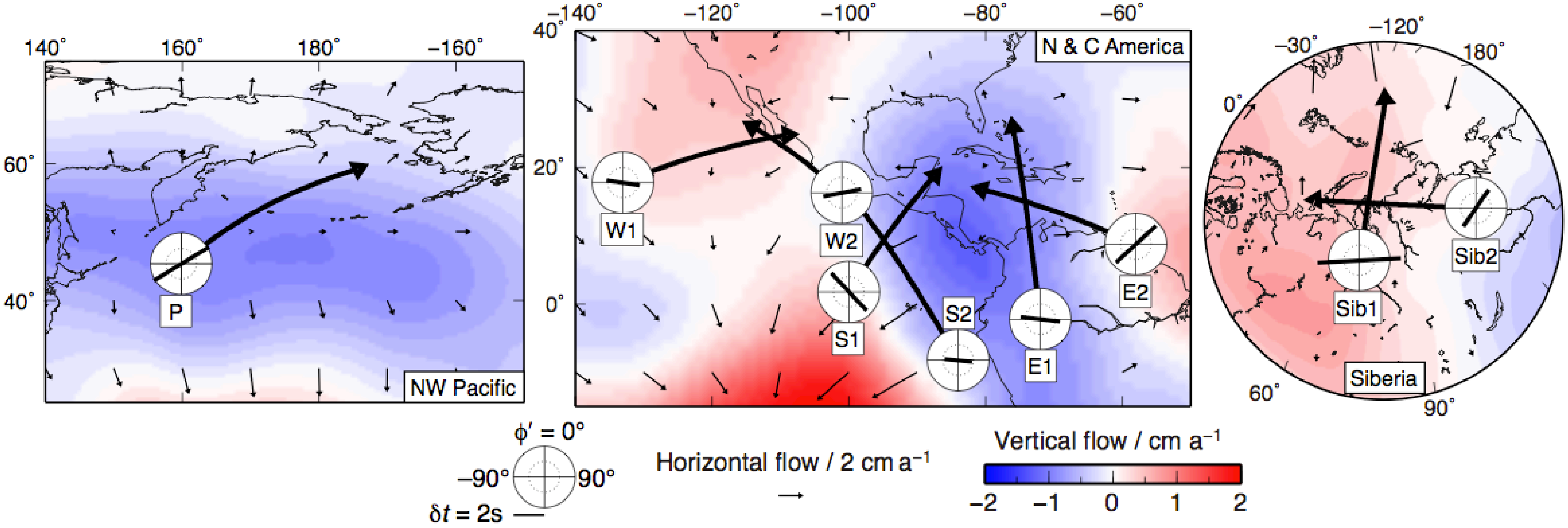

Conclusions

- In general, the lowermost mantle is anisotropic, but clear regional variations are evident.
- Anisotropy is the fingerprint of D” mineralogy and style of deformation.
- Compared observations with numerical predictions from linked flow and LPO modelling.
- Three different plasticity cases for dislocation creep in ppv are considered, with that favouring slip on (010) matching best (at least in regions of subduction).

Future Directions

- More observations – global dataset
- Full waveform modelling – how important are finite-frequency effects?
- To what degree do dynamic recrystallisation, work hardening, climb and the presence of other phases change the texture?
- What are the effects of inherited petrofabric textures (e.g, pv to ppv)?
- Effects of melt
- Is LPO in post-perovskite important everywhere in D” - do other anisotropy generating processes play a role?

University of
BRISTOL

Towards better data coverage

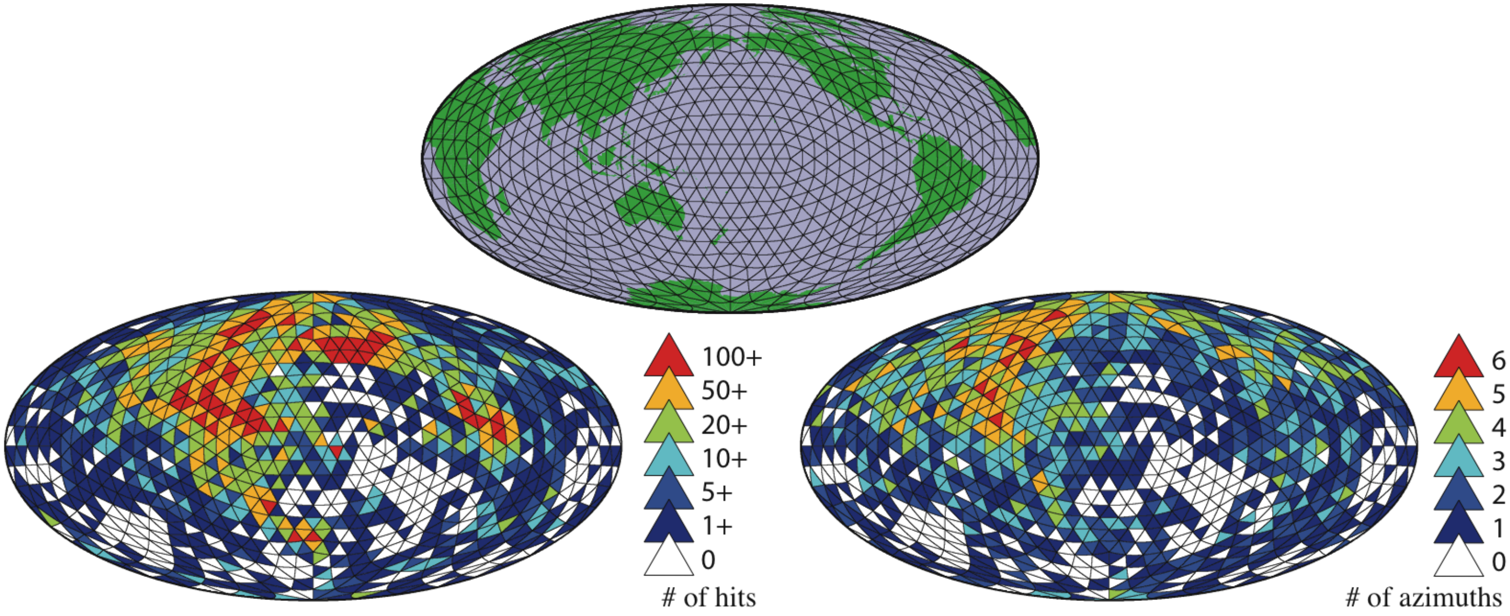

Image courtesy of Jack Walpole